

Estimation of extra-tropical air-sea temperature differences

K. J. Wilson and S. C. Martin, Head Office, Bureau of Meteorology, Melbourne
(Manuscript received March 1983; revised September 1983)

Regression equations for the extra-tropical air-sea temperature difference were tested. The predictors used were parameters available from satellite retrievals or through the interpretation of satellite imagery. A simple model was used to physically relate the predictors and predictand where necessary. The results were primarily dependent on the sign of the surface pressure anomaly. A correlation of 0.7 with a standard error of estimate of 1.1K was found in areas of negative surface pressure anomaly. In regions of positive surface pressure anomaly the relative invariance of the air-sea temperature difference combined with the difficulty of adequately allowing for subsidence inversions resulted in a weaker correlation.

Introduction

The paucity of observations over the extensive ocean areas of the southern hemisphere is consistently cited as a major factor limiting the quality of numerical and manual prognoses in that region. Studies designed to evaluate the impact of observations additional to the conventional data base have shown that southern hemisphere analyses and prognoses benefit significantly from the inclusion of ocean buoy data and satellite temperature retrievals (for example Guymer and Le Marshall 1980; Gauntlett and Leslie 1982). The improvements found are generally greater than those resulting from the inclusion of similar data in northern hemisphere studies (Ohring 1979), presumably due to the greater initial data deficiency south of the equator. The specification of additional meteorological fields over the ocean is thus particularly important in the southern hemisphere and there is a general awareness that such information must necessarily be derived from remote sensing systems.

Routine inclusion of temperature profiles obtained from satellite retrieval techniques should alleviate the initial state specification problem to some extent, but a remaining area of particular difficulty is the derivation of surface winds, temperatures and pressures. Inclusion of surface winds and pressures particularly have been shown to lead to improved analyses and resultant prognoses (Cane et al. 1981; Guymer and Le Marshall 1980). In the absence of routine surface wind estimates, such as those provided by SEASAT, it is likely that surface winds will be derived through conversion factors from either surface geostrophic winds (Hasse and Wagner 1971) if the pressure distribution is known, or from low-level cloud vectors (Zank 1981). In either case, the conversion factors will depend primarily on low-level stability and baroclinicity, both of which are related to the low-level temperature distribution. Satellite derived temperature profiles do not have sufficient vertical resolution to provide reliable

estimates of near-surface lapse rates. Horizontal gradients, while more reliable, tend to be underestimated, particularly in the southern hemisphere (Gruber and Watkins 1982). In this paper, statistical relationships between the air-sea temperature difference and other routinely available meteorological parameters are considered. The air-sea temperature difference was chosen because there are reasons for expecting this parameter to correlate with other more amenable variables (Zillman and Price 1972); it provides a direct estimate of low-level stability (e.g. Hasse and Wagner 1971); and coupled with satellite derived sea surface temperatures it could provide estimates of surface air temperature which, if included in retrieval regression procedures, would be expected to improve the low-level variance characteristics and error statistics of the satellite temperature profiles (Phillips 1981).

The approach used draws on the work of Guymer (1978) and Zillman and Price (1972). Following the proposal of Taljaard and van Loon (1960), which was based on the classical relationship between surface pressure features and the three-dimensional temperature distribution, Guymer (1978) has described a technique for quantifying satellite imagery in terms of the 1000-500 mb thickness anomaly. The results of Zillman and Price (1972), however, suggested that cloud features in mid-latitude cyclones could also be related to lower tropospheric layer-mean lapse rates and to the air-sea temperature difference. As the cloud distribution is common to both approaches, there is a possibility of significant cross-correlation between the thickness anomaly and the layer-mean lapse rate and air-sea temperature difference. Inspection of the results of Zillman and Price (1972) confirmed the likelihood of a significant relationship and the present work is intended firstly to establish a physical basis for the correspondence between lapse rates, air-sea temperature difference and the cloud distribution

and then to quantify the relationship between thickness anomaly, lapse rate and air-sea temperature difference as a means of determining the latter.

The simple model

The equations of motion for horizontal frictionless flow in isentropic co-ordinates can be combined under the dry adiabatic assumption $d\theta/dt = 0$ to give the isentropic vorticity equation

$$\frac{d}{dt}(\zeta_\theta + f) = -(\zeta_\theta + f)\nabla_\theta \cdot \underline{V} \quad \dots 1$$

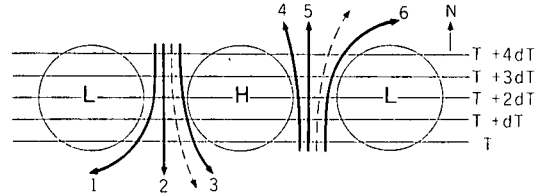
where ζ_θ and $\nabla_\theta \cdot \underline{V}$ are the relative vorticity and divergence respectively derived from the horizontal wind field on an isentropic chart (e.g. Haltiner and Martin 1957). Substituting the continuity equation in isentropic co-ordinates into Eqn 1 and applying the resultant equation to two isentropes separated vertically by a pressure difference Δp gives the equation for conservation of potential vorticity

$$\frac{\zeta_\theta + f}{\Delta p} = \text{constant} \quad \dots 2$$

It follows from Eqn 2 that any latitudinal displacement of a column of air can be compensated for by a change in its relative vorticity, a change in the pressure spacing between isentropes or both.

Figure 1 shows an idealised distribution of mean sea level (MSL) pressure systems in the southern hemisphere. The trajectories of eight air columns are also shown. If it is assumed that each column initially has zero relative vorticity then application of Eqn 2 to trajectory 1, for example, indicates that as the column moves poleward and acquires cyclonic (negative) relative vorticity, reflected here by cyclonic curvature, $(\zeta_\theta + f)$ increases in magnitude implying a proportional increase in Δp . Given the constraint of a solid lower boundary, this process must be associated with ascent and a decrease in $\partial\theta/\partial p$ between the relevant isentropes. This implies that the air column becomes more unstable as it progresses along trajectory 1. Application of this argument to

Fig. 1 Idealised distribution of mean sea level pressure in the southern hemisphere. Dashed lines represent trajectories along which the change in relative vorticity exactly cancels the change in Coriolis parameter. Stability tendencies for air columns moving along trajectories 1 to 6 are given in Table 1. Idealised sea surface isotherms are also shown (thin lines, $dT > 0$).



each of the six numbered trajectories in Fig. 1 gave the stability tendencies in Table 1 ranging from strong destabilisation along trajectory 1 to strong stabilisation along trajectory 4. More details on this process are provided by Palmen and Newton (1969).

Equation 2 has obvious limitations. Over an extended period diabatic effects such as surface fluxes, radiation and latent heat release will invalidate the dry adiabatic assumption and significant departures might be expected. Despite these limitations, however, Palmen and Newton (1969) show that this equation provides a useful basis for understanding the typically observed free tropospheric thermal structure in mid-latitude synoptic systems. In terms of the present application, however, it is necessary to consider the correction arising from the modification of low-level lapse rates by surface fluxes. It is well known that extra-tropical oceanic near-surface lapse rates correlate strongly with air-sea temperature differences and in turn with the surface heat fluxes through the bulk aerodynamic relationships. It is probable then that low-level lapse rates are determined more by the surface flux than by the constant potential vorticity argument outlined above. As an extension of the argument, an idealised sea surface temperature distribution, with warmer water toward the equator and progressively cooler water poleward, was superimposed on the MSL pattern in Fig. 1. The bulk aerodynamic equation for the surface heat flux H is

Table 1. Stability tendencies in the free troposphere and boundary layer for atmospheric columns moving along the trajectories of Fig. 1. Columns may become very unstable (VU), unstable (U), stable (S) or very stable (VS).

Trajectory	Free troposphere	Boundary layer
1	VU	S
2	U	S
3	S	S
4	VS	U
5	S	U
6	U	U

$$H = \rho C_p C_H V (T_{ss} - T_{sa}) \quad \dots 3$$

where the speed of the sea surface has been assumed negligible and ρ is the air density, C_p the specific heat of air at constant pressure, C_H the bulk heat transfer coefficient, V the surface wind speed and T_{ss} and T_{sa} are the sea surface and surface air temperatures respectively. A positive, or surface to air, heat flux ($T_{ss} > T_{sa}$) is associated with an unstable boundary layer. The equatorward trajectories in Fig. 1 represent the passage of relatively cold air over a warm sea surface and would be associated with a surface to air heat flux and low-level instability. Along the poleward trajectories the heat flux is directed from the air to the relatively cool sea surface and the boundary layer is stably stratified. The low-level stability along each of the numbered trajectories in Fig. 1 is given in Table 1.

Combining the boundary layer and free tropospheric stability tendencies along each of the trajectories from Table 1, and given the sign of the vertical motion, it was then possible to outline the expected cloud distribution. Along trajectories 1 and 2, the stable boundary layer and unstable free troposphere will be associated with middle-level cloud layers. Subsidence and an air to surface heat flux along trajectory 3 indicates clear skies, fog or stratus depending in part on the low-level wind structure. The likelihood of a strong subsidence inversion and an unstable boundary layer is indicative of stratocumulus fields for trajectory 4 while the weaker subsidence along trajectory 5 will allow shallow cumuliform cloud. Ascent combined with a surface to air heat flux makes trajectory 6 favourable for deep convective development. While the details of the cloud distribution will also depend, for example, on the moisture availability, the diagnosed distributions are broadly representative of what is routinely observed, lending some support to the utility of this simple model.

The model indicates that both the near-surface and mid-tropospheric stabilities have a role in determining the cloud distribution. In this context it should be noted that the free tropospheric stability is determined largely by the absence or presence and strength of shallow subsidence inversions capping the boundary layer rather than by the lapse rate above the inversion (e.g. Zillman and Price 1972). From the viewpoint of developing regression relations for the air-sea temperature difference based on satellite derived data, the importance of these two shallow regions is unfortunate. The vertical resolution of current satellite retrieval systems is poor, particularly in the lower troposphere and accurate determination of the lapse rates specifically in these two layers is not possible. An alternative is to combine the near-surface and free tropospheric stability characteristics into a single parameter which can be remotely determined. One such parameter is the layer-mean lapse rate devised by Zillman and Price (1972). This lapse rate is defined such that a temperature profile

constructed from it and the sea surface temperature alone will conserve energy between the surface and upper reference level (700 or 500 mb here) relative to the environmental trace. An example is shown in Fig. 2. So defined, the layer-mean lapse rate can be obtained with reasonable accuracy from satellite data as mid-tropospheric temperatures are well determined and sea surface temperatures can be estimated to within 1°C and are more reliable than surface air temperature estimates (e.g. Saunders et al. 1982; Gruber and Watkins 1982). The ability of the mean lapse rate to differentiate between the varying stability regimes along the trajectories in Table 1 is illustrated in Fig. 3. Idealised temperature profiles referenced to a common surface temperature are given for trajectories 1, 4 and 6 of Fig. 1 and the corresponding layer-mean lapse rates are also shown. These idealised profiles are similar to the mean observed profiles for the corresponding cloud regimes given by Zillman and Price (1972) and comparison of the layer-mean lapse rates for trajectories 1 and 6 and 4 and 6 shows the respective influences of the near-surface and mid-tropospheric (as reflected in the strength of the subsidence inversion) stabilities. These two aspects of the simple model can then be combined into a single parameter which can be remotely determined and conversely the simple model provides some physical basis for the relationship between the cloud distribution and the layer-mean lapse rate found by Zillman and Price (1972). The rationale for relating satellite imagery to thickness anomalies is already embodied in the classical model of mid-latitude cyclones.

Fig. 2 The layer-mean lapse rate between the surface and an upper reference level was found as $(T_m - T_{ss})/\ln(P_2/P_1)$ where $P_{1,2}$ are the surface and reference level pressures (1002 mb and 500 mb here) respectively and T_m is the temperature at P_2 chosen such that the area A = area B on a skew T — ln p diagram. The heavy line is the environmental temperature trace.

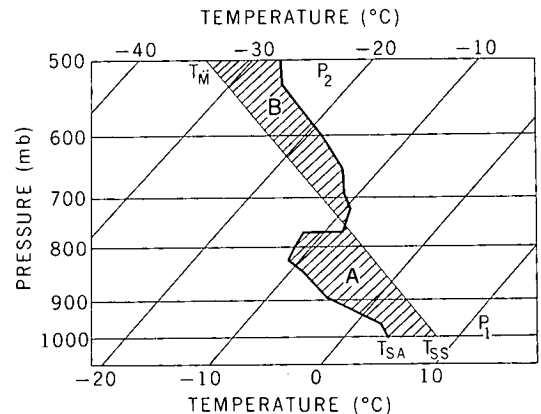
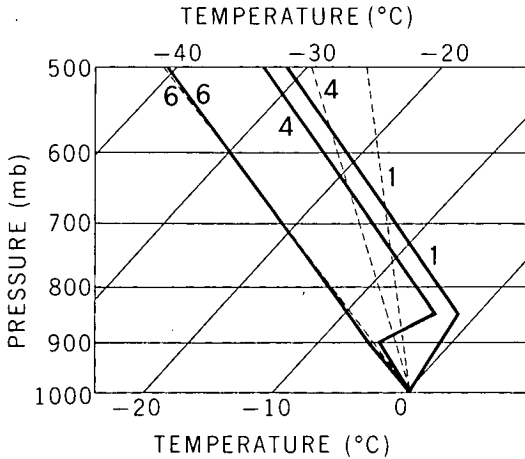


Fig. 3 Idealised temperature profiles (solid lines) for trajectories 1, 4 and 6 of Fig. 1, referenced to a common surface temperature and assuming $T_{ss} = T_{sa}$. The profile constructed using the layer-mean lapse rate (dashed line) is also shown for each case.



Data and Method

The data used in this study were drawn from the meteorological observations taken by the Antarctic research vessel, USNS *Eltanin*. The meteorological activities of the *Eltanin*, including details of measurements made and observation techniques, have been summarised by Zillman and Dingle (1973). During the six cruises referred to, each of approximately two months duration (Table 2), routine 2300 GMT radiosonde observations were taken as well as six-hourly surface observations, including sea surface temperature. In some cases, 1100 GMT radiosonde observations were also taken. Overall, 417 radiosonde observations with simultaneous surface data were available.

Air-sea temperature differences, layer-mean lapse rates and thickness anomalies were computed from the observations, with anomalies found as deviations from the climatic mean data of Taljaard et al. (1969).

The data cover all seasons but are geographically biased toward middle and high latitudes in the southeastern Pacific and waters to the south of Australia (Fig. 4).

The cloud distribution appears to be significantly related to both the thickness anomaly ϕ (Guymer 1978) and the layer-mean lapse rate γ (Zillman and Price 1972). Further, the layer-mean lapse rate is dependent on both the near-surface lapse rate, and hence the air-sea temperature difference, and the mid-tropospheric stability. Given the existence of these relationships and following inspection of the results of Zillman and Price (1972) a regression relation for the air-sea temperature difference of the form

$$T_{sa} - T_{ss} = a + b\gamma + c\phi \quad \dots 4$$

was sought with γ found as $\partial T / \partial (\ln p)$ and where a, b, c are regression constants. Standard SI units were adopted for each parameter. Equation 4 includes some redundancy due to the contribution of $(T_{sa} - T_{ss})$ to γ but has the advantage that the predictors can be estimated from remotely sensed data.

Multiple linear regressions were performed over the whole data set as well as over subsets according to latitude, season, time of day, cruise number and surface pressure anomaly. All correlation coefficients were tested for statistical significance at the 99.5 per cent interval of the t-test.

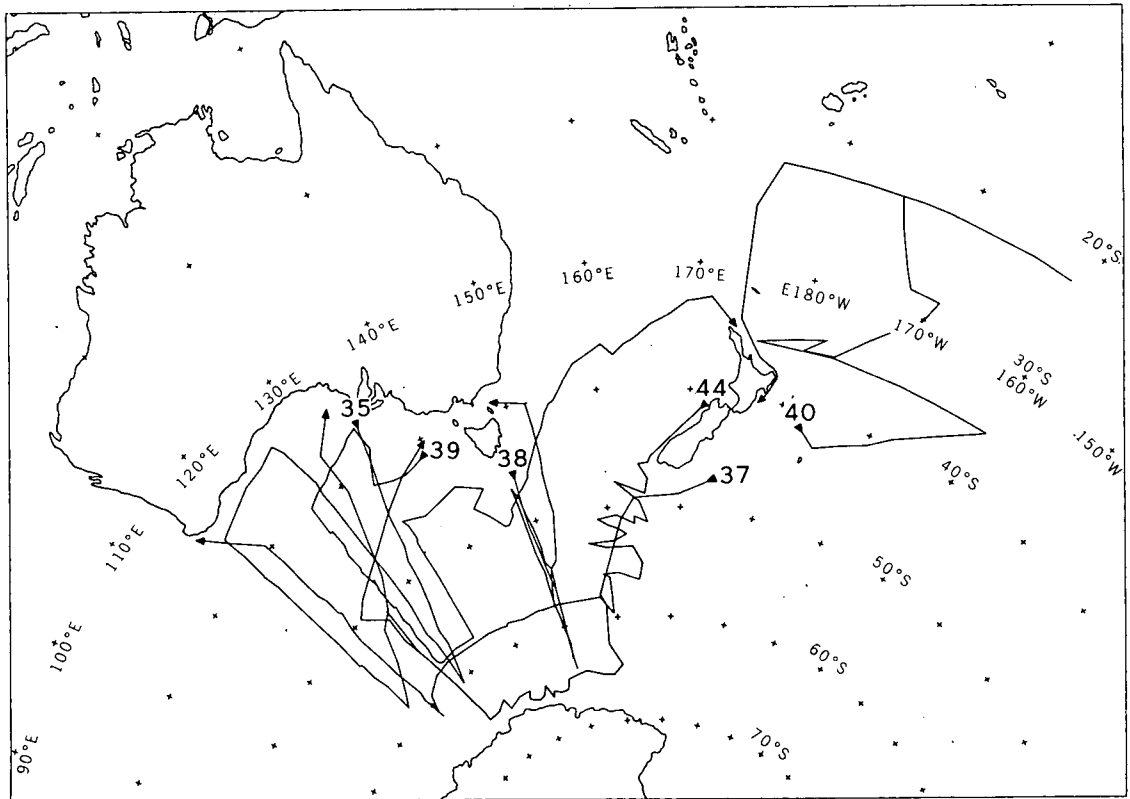
Results

The regression procedure revealed no significant differences between different cruises or between 1100 and 2300 GMT data. Correlation coefficients obtained for regressions over all data are given in Table 3 for the layers 1000 — 700 mb and 1000 — 500 mb and are statistically significant. Division of the data into two subsets according to the sign of the surface pressure anomaly resulted in two significantly different regression equations (Table 3). The percentage of the variance explained increased in areas of negative surface pressure anomaly but

Table 2. Data from the USNS *Eltanin* used in this study.

Cruise number	Dates	Number of radiosondes and simultaneous sea surface temperatures available	
		1100 GMT	2300 GMT
35	12 Aug — 8 Oct 1968	0	55
37	10 Jan — 3 Mar 1969	0	49
38	20 Mar — 13 May 1969	34	51
39	8 Jun — 5 Aug 1969	43	49
40	15 Sep — 21 Nov 1969	0	59
44	24 Jun — 18 Aug 1970	23	54

Fig. 4 Track of the USNS Eltanin during the six cruises which provided the data for this study.



decreased in regions of positive surface pressure anomaly, although the correlation remained statistically highly significant. Variations in correlation were also found with season and latitude but these were primarily attributable to associated changes in the relative frequency of positive and negative surface pressure anomalies. The weaker correlation in regions of positive surface pressure anomaly stemmed partly from difficulties in adequately capturing the effect of subsidence inversions. Also, the temperature difference between the air and sea surface is less variable in these areas.

In addition to the multiple linear regression, simple regressions were also tested with b or c assumed zero in Eqn 4 in order to isolate contributions from γ and ϕ to the regression. The result for regressions over all data are given in Table 4 and show that little additional information was gained by including both γ and ϕ in the regression. Regressions based on ϕ alone explained only marginally less variance over the 1000 — 500 mb layer but γ was the superior single predictor particularly for the shallower layer. In all cases the standard error of estimate associated with the regression was between 0.9 and 1.3K. For a typical range of thickness anomalies (Guymer 1978) and layer-mean lapse rates (Zillman and Price 1972) the regression equations predict values of $T_{sa} - T_{ss}$ ranging from approximately -4.5K to 1.5K, in broad

agreement with the range given by Zillman and Price (1972).

Discussion

In the simple model presented earlier, the broadscale cloud distribution was related to the expected vertical motion and air-sea temperature difference. The effect of the vertical motion on atmospheric stability was then used as a basis for including the layer-mean lapse rate γ as a predictor in Eqn 4. Division of the data into two groups depending on the sign of the surface pressure anomaly revealed that difficulties arose partly in the presence of subsidence inversions. The lapse rate has the advantage of being easily determined but in view of the problem associated with its use, vertical motion was tested as an alternative predictor. Vertical velocities were computed from the single-station ship observations based on the equation

$$w = \frac{\frac{\partial T}{\partial t} + \frac{fT}{g} \left(v \frac{\partial u}{\partial z} - u \frac{\partial v}{\partial z} \right) + \frac{Q}{C_p}}{(\gamma_d - \gamma_e)} \quad \dots 5$$

where u , v , w are the x (eastward), y (northward) and z components of motion ($m s^{-1}$); t is time; T the

Table 3. Regression parameters for the multiple linear regression expressed by Eqn 3. The correlation coefficient (r), standard error of estimate (σ) and regression constants (a , b , c) are given for regressions over all data and subsets representing positive and negative surface pressure anomalies. Predictors were evaluated for the 1000–700 mb and 1000–500 mb layers.

	r	σ	1000–500 mb			r	σ	1000–700 mb		
			a	b	c			a	b	c
All data	0.61	1.2	1.90	-0.0589	0.0067	0.70	1.1	1.668	-0.0505	0.0063
Positive surface pressure anomaly	0.50	1.2	1.078	-0.0460	0.0056	0.60	1.1	1.082	-0.0422	0.0038
Negative surface pressure anomaly	0.74	1.1	4.253	-0.0998	0.0051	0.81	0.9	2.870	-0.0678	0.0054

Table 4. As for Table 3 but b or c assumed zero. Regression over all data.

	r	σ	$b=0$		r	σ	$c=0$	
			a	c			a	b
1000–700 mb	0.56	1.2	-1.206	0.0288	0.70	1.1	2.099	-0.0579
1000–500 mb	0.53	1.3	-0.966	0.0149	0.58	1.2	3.006	-0.0824

Table 5. As for Table 3 but regression over those data for which vertical velocities are defined. Results are included for two sets of predictors; (ϕ, γ) and (ϕ, w) .

	r	σ	(ϕ, γ)			r	σ	(ϕ, w)		
			a	b	c			a	b	c
1000–700 mb	0.68	0.9	1.889	-0.0489	0.0087	0.68	0.9	-1.392	18.901	0.0199
1000–500 mb	0.56	1.0	2.282	-0.0610	0.0048	0.68	0.9	-1.257	20.599	0.0108

temperature; f the Coriolis parameter; g gravity; Q the rate of diabatic heating per unit mass and γ_d, γ_e the dry adiabatic and environmental lapse rates respectively, after Tucker (1973). Equation 5 derives from the first law of thermodynamics and the approximations required to reach this form are given by Tucker. The diabatic heating was assumed here to result solely from radiation effects and the Q profile adopted by Tucker (1973) was employed. As only the single-station ship observations were available here the problems of estimating a latent heat contribution to Q or assessing the degree of synoptic-scale saturation as a criterion for modifying the denominator in Eqn 5 to $(\gamma_s - \gamma_e)$, where γ_s is the saturated adiabatic lapse rate, were greatly magnified. Accordingly moist processes were neglected in this trial calculation.

Tucker (1973) investigated the impact of temporal and vertical observational resolution on the derived vertical motion and for standard level data reported at 12-hourly intervals, the results indicated that only layer-mean values might be representative. Radar wind observations necessary to evaluate the right hand side of Eqn 5 were available 12-hourly at standard levels only from cruise 39 of the *Eltanin*. The observation resolution was elsewhere even poorer. Equation 5 was modified to allow for the motion of the ship and used to compute layer-mean vertical velocities for the surface — 700 mb and surface — 500 mb layers. The resultant values were then used in Eqn 4, rather than γ , and the regression parameters are presented in Table 5. Values obtained using Eqn 4 on the same subset of data are also given. For this limited test, which included a greater than

average proportion of positive surface pressure anomaly cases, the results using vertical motion were superior over the 1000-500 mb layer to those based on the layer-mean lapse rate. The limited data set and the approximations used in computing w indicate that this result should be treated with caution. Further testing of this alternative, however, appears warranted although the technique used to find w should be independent of the analysis (e.g. Shenk 1963).

The sea surface temperature alone was found to explain approximately 95 per cent of the variance in the surface air temperature in this study. This was due to the marked latitudinal trend in both surface temperatures and explains to some extent why sea surface temperatures are often employed as approximations to the surface air temperature when the latter are not available. However, air-sea temperature differences of up to 10K might be expected in extreme cases over open ocean and this difference varies systematically across extra-tropical synoptic systems (e.g. Zillman and Price 1972). The absence of systematic forcing of this magnitude from, for example, regression procedures used in constructing satellite temperature profiles, would be expected to have some impact, particularly if sea surface temperatures are used as a *de facto* lower boundary condition. The absence of this effect could be one cause for the finding that the variance in southern hemisphere mid-latitude 1000 — 850 mb mean temperature analyses derived from satellite soundings may be only 60 per cent of that based on routine observations (Gruber and Watkins 1982), although part of this discrepancy results from the regression procedure used in processing the satellite data (McMillin and Dean 1982). The results presented here indicate that, given a thickness anomaly and layer-mean lapse rate, the air-sea temperature difference can be obtained statistically with a standard error of estimate of 1.1K. It should be noted, however, that operational estimates could be less accurate due to the reduced accuracy of both the sea surface temperatures and the thickness field in that environment. Further work on the inclusion of vertical motion as a predictor may offset any such reduced accuracy.

Summary

Regression equations for predicting the difference between the surface sea and air temperatures were tested. The predictors were required to be available from satellite temperature retrievals or through the quantitative interpretation of satellite imagery. A simple theoretical model, with empirical support, was used to physically relate the vertical velocity and the air-sea temperature difference, or layer-mean lapse rate, to the observed cloud distribution and hence to thickness anomalies. The results were primarily dependent on the sign of the surface pressure anomaly. Thickness anomaly and layer-mean lapse

rate combined were found to predict the air-sea temperature difference with a standard error of estimate of 1.1K and a multiple correlation coefficient of 0.7 in areas of negative surface pressure anomaly. In regions of positive surface pressure anomaly, the prevalence of subsidence inversions and reduced variability in $T_{sa} - T_{ss}$ resulted in a weaker correlation. Limited tests suggested that this might be overcome by replacing the layer-mean lapse rate with the layer-mean vertical velocity as a predictor. The use of the layer-mean lapse rate as the sole predictor gave only marginally less satisfactory results. The results obtained suggest that these statistical relationships would be adequate for determining the broadscale distribution of boundary layer stability required in deriving surface winds from geostrophic or cloud motion vectors. Contributions of baroclinicity to the change in wind with height in the boundary layer might also be more accurately delineated if the regression relationships were used to provide lower boundary conditions for maritime extra-tropical satellite temperature retrievals and a limited test of this procedure in an analysis scheme appears warranted.

Acknowledgments

The authors wish to thank Messrs C. Giblin and D. Dargan for extracting the data. Mr I. Bell suggested combining the boundary layer stability argument with conservation of potential vorticity as proposed in the simple physical model.

References

- Cane, M. A., Cardone, V. J., Halem, M. and Halberstam, I. 1981. On the sensitivity of numerical weather prediction to remotely sensed marine surface wind data: A simulation study. *J. geophys. Res.*, **86**, 8093-106.
- Gauntlett, D. J. and Leslie, L. M. 1982. Current status and future prospects for numerical weather prediction — an Australian perspective. *Aust. Met. Mag.*, **30**, 57-68.
- Gruber, A. and Watkins, C. D. 1982. Statistical assessment of the quality of TIROS-N and NOAA-6 satellite soundings. *Mon. Weath. Rev.*, **110**, 867-76.
- Guymer, L. B. 1978. Operational application of satellite imagery to synoptic analysis in the southern hemisphere. *Tech. Rep. 29*, Bur. Met., Australia, 83 pp.
- Guymer, L. B. and Le Marshall, J. F. 1980. Impact of FGGE buoy data on southern hemisphere analysis. *Aust. Met. Mag.*, **28**, 19-42.
- Haltiner, G. J. and Martin, F. L. 1957. *Dynamical and Physical Meteorology*. McGraw-Hill, New York, 470 pp.
- Hasse, L. and Wagner, V. 1971. On the relationship between geostrophic and surface wind at sea. *Mon. Weath. Rev.*, **99**, 255-60.
- McMillin, L. M. and Dean, C. A. 1982. Variance ratios, loss of energy and regression in satellite temperature retrievals. *Mon. Weath. Rev.*, **110**, 296-9.
- Ohring, G. 1979. Impact of satellite temperature sounding data on weather forecasts. *Bull. Am. met. Soc.*, **60**, 1142-7.
- Palmen, E. and Newton, C. W. 1969. *Atmospheric Circulation Systems*. Academic Press, New York, 603 pp.
- Phillips, N. A. 1981. Cloudy winter satellite temperature retrievals over the extratropical northern hemisphere oceans. *Mon. Weath. Rev.*, **109**, 652-9.

- Saunders, R. W., Ward, N. R., England, C. F. and Hunt, G. E. 1982. Satellite observations of sea surface temperature around the British Isles. *Bull. Am. met. Soc.*, 63, 267-72.
- Shenk, W. E. 1963. TIROS II window radiation and large scale vertical motion. *Jnl appl. Met.*, 2, 770-5.
- Taljaard, J. J. and van Loon, H. 1960. The construction of 500 mb contour maps over the Southern Ocean. *Proc. Symposium on Antarctic Meteorology, Melbourne*. Pergamon Press, pp. 96-114.
- Taljaard, J. J., van Loon, H., Crutcher, H. L. and Jenne, R. L. 1969. *Climate of the upper air. Southern Hemisphere. Vol 1*. ESSA Environmental Data Service.
- Tucker, G. B. 1973. Vertical velocities and vertical eddy fluxes derived from serial soundings at one station. *Q. Jl R. met. Soc.*, 99, 520-39.
- Zank, S. 1981. Sea surface winds derived from cloud motion vectors over the tropical Atlantic. *Bound. Lay. Met.*, 19, 223-33.
- Zillman, J. W. and Dingle, W. R. J. 1973. Meteorology. *Antarctic Journal of the United States*, 8, 111-9.
- Zillman, J. W. and Price, P. G. 1972. On the thermal structure of mature Southern Ocean cyclones. *Aust. Met. Mag.*, 20, 34-48.